Current results from AIRS/AMSU/HSB

Joel Susskind[a], Robert Atlas[a], Christopher Barnet[b], John Blaisdell[c], Lena Iredell[c], Genia Brin[c], Juan Carlos Jusem[c], Fricky Keita[c], Louis Kouvaris[c], Gyula Molnar[b]

[a]NASA Goddard Space Flight Center, Greenbelt, MD, USA 20771

[b]Joint Center for Earth Systems Technology, NASA GSFC, Greenbelt, MD, USA 20771

[c]Science Applications International Corporation, NASA GSFC, Greenbelt, MD, USA 20771

Abstract

AIRS was launched on EOS Aqua on May 4, 2002, together with AMSU A and HSB, to form a next generation polar orbiting infrared and microwave atmospheric sounding system. The primary products of AIRS/AMSU/HSB are twice daily global fields of atmospheric temperature-humidity profiles, ozone profiles, sea/land surface skin temperature, and cloud related parameters including OLR. The sounding goals of AIRS are to produce 1 km tropospheric layer mean temperatures with an rms error of 1K, and layer precipitable water with an rms error of 20%, in cases with up to 80% effective cloud cover. Pre-launch simulation studies indicated that these results should be achievable. Minor modifications have been made to the pre-launch retrieval algorithm as alluded to in this paper. Sample fields of parameters retrieved from AIRS/AMSU/HSB data are presented and temperature profiles are validated as a function of retrieved fractional cloud cover. As in simulation, the degradation of retrieval accuracy with increasing cloud cover is small. Select fields are also compared to those contained in the ECMWF analysis, done without the benefit of AIRS data, to demonstrate information that AIRS can add to that already contained in the ECMWF analysis. Assimilation of AIRS temperature soundings in up to 80% cloud cover for the month of January 2003 into the GSFC FVSSI data assimilation system resulted in improved 5 day forecasts globally, both with regard to anomaly correction coefficients and the prediction of location and intensity of cyclones.

Introduction

AIRS/AMSU/HSB is a state of the art advanced infra-red microwave sounding system that was launched on the EOS Aqua platform in a 1:30 AM/PM sun synchronous orbit on May 4, 2002. An overview of the AIRS instrument is given in Pagano et al[1]. The sounding goals of AIRS are to produce 1 km tropospheric layer mean temperatures with an rms error of 1K, and layer precipitable water with an rms error of 20%, in cases with up to 80% effective cloud cover. Aside from being part of a climate mission, one of the objectives of AIRS is to provide sounding information of sufficient accuracy such that when assimilated into a general circulation model, significant improvement in forecast skill would arise. The pre-launch algorithm to produce level 2 products (geophysical parameters) using AIRS/AMSU/HSB data, and expected results based on simulation studies, are given in Susskind et al.[2] The results of that simulation indicate that the sounding goals of AIRS/AMSU/HSB should be achievable. In that simulation, perfect knowledge of the instrumental spectral response functions and the inherent physics of the radiative transfer equations was assumed. Therefore, if the true state of the atmosphere and underlying surface were known perfectly, one could compute the radiances AIRS, AMSU, and HSB would see exactly up to instrumental noise. Susskind

et al.[2] alluded to the fact that this is not the case but in reality, and additional terms would have to be included in the retrieval algorithm to account for systematic differences (biases) between observed brightness temperatures and those computed knowing the "true" surface and atmospheric state, as well as residual computational errors after that systematic bias is accounted for (computational noise). In this paper, we show results based on the algorithm we were using to analyze AIRS/AMSU/HSB data on June 30, 2003, which we will refer to as Version 3.1. This algorithm is very similar to the pre-launch version, with the major differences attributable to the factors described above. JPL delivered an earlier version of the algorithm, Version 3.0, to the Goddard DAAC, for the earliest near real time processing of AIRS level 2 products starting in August 2003. We have used Version 3.1 to analyze data for the AIRS focus day September 6, 2002, and all of January 2003 for use in a forecast impact experiment. Research to further improve the results of analysis of AIRS/AMSU/HSB data is continuing. JPL plans to deliver an improved version to the DAAC in the Spring of 2004 to be used to process near real time AIRS data from that point forward, as well as reprocess all AIRS data from September 2002, when the instrument became stable.

Overview of the AIRS Team Retrieval Algorithm

The AIRS team retrieval algorithm is basically identical to that described in Susskind et al.[2] The key steps are outlined below: 1) Start with an initial state consistent with the AMSU A and HSB radiances[3]; 2) Derive IR clear column radiances $\hat{R}_i^0$ valid for the 3x3 AIRS Fields of View (FOVs) within an AMSU A Field of Regard (FOR) consistent with the observed radiances and the initial state; 3) Obtain an AIRS regression guess[4] consistent with $\hat{R}_i^0$ using 1504 AIRS channels; 4) Derive $\hat{R}_i^1$ consistent with the AIRS radiances and the regression guess; 5) Derive all surface and atmospheric parameters using $\hat{R}_i^1$ for 415 AIRS channels and all AMSU and HSB radiances; 6) Derive cloud parameters and OLR consistent with the solution and observed R_i; 7) Apply quality control, which rejects a solution if the retrieved cloud fraction is greater than 80% or other tests fail. In the event that a retrieval is rejected, cloud parameters are determined using the initial microwave state and observed AIRS radiances. Figure 1 shows a typical AIRS spectrum and indicates by different colors the AIRS channels used in different retrieval steps which are performed sequentially.

Results Using Version 3.1

Figure 2 shows the number of cases for each retrieved effective fractional cloud, in 0.5% bins, for the whole day September 6, 2002. The effective fractional cloud cover is given by the product of the fraction of the field of view covered by clouds and the cloud emissivity at 11 μm. The average global effective cloudiness was determined to be 38.26%. Also shown is the percent of accepted retrievals as a function of retrieved effective cloud cover. Roughly 93% of the cases with retrieved effective cloud cover 20% were accepted, falling to 63% at 60% effective cloud cover, and to 45% at 80% effective cloud cover. All cases with retrieved effective cloud cover greater than 80% are rejected.[2] The average effective fractional cloudiness for all accepted cases was 27.06%. These results are very similar to what was shown in the simulation study.[2]

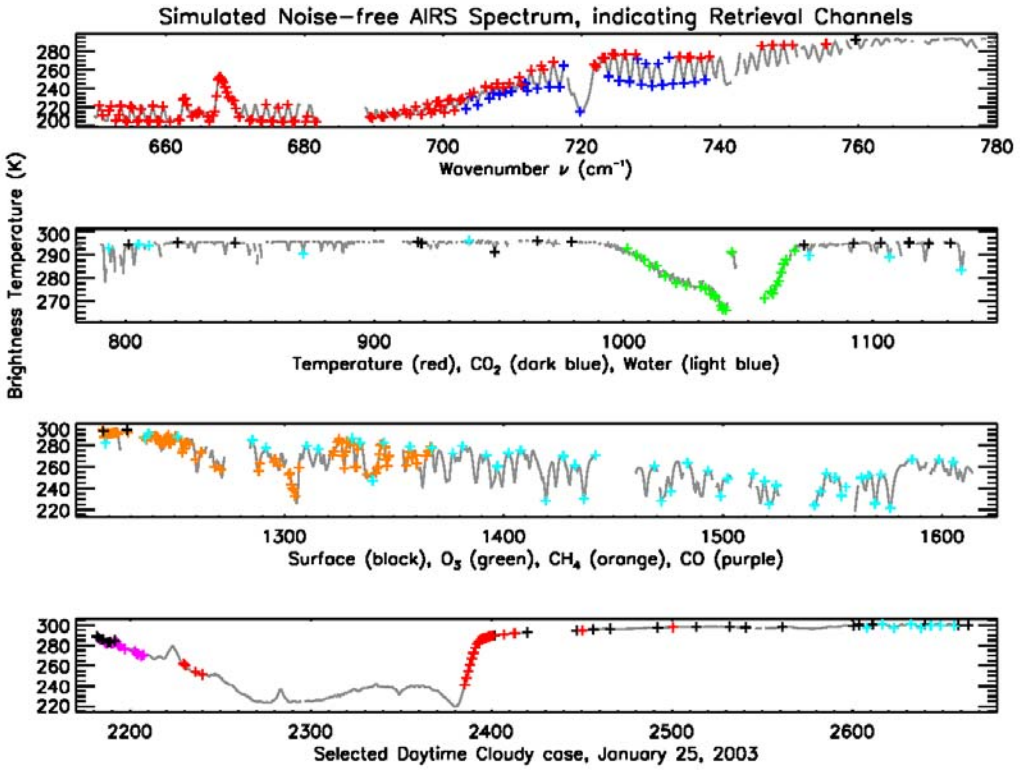

Figure 1

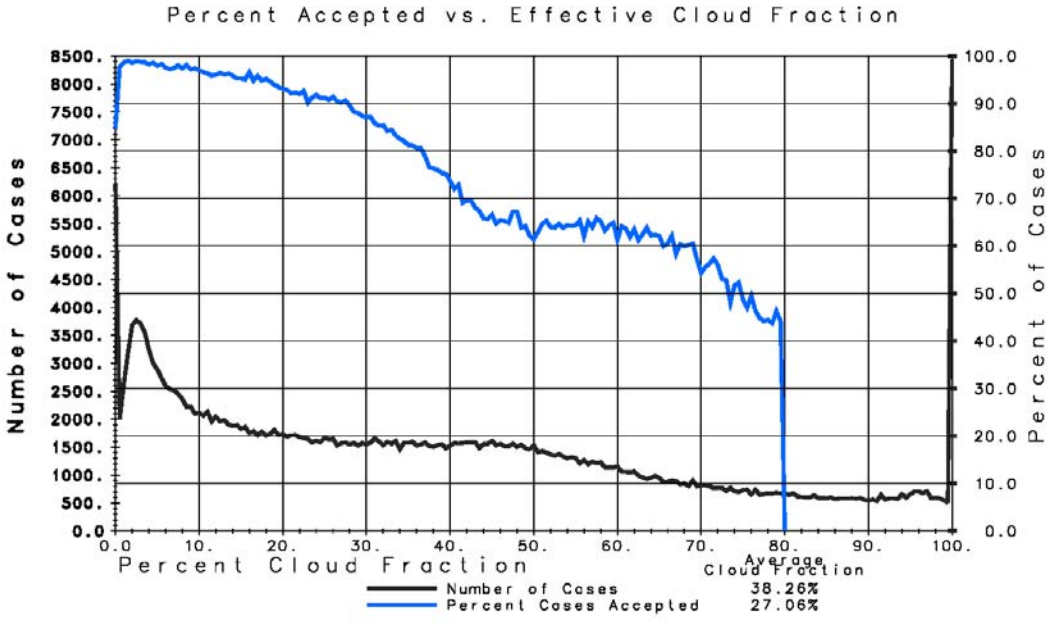

Figure 2

Figure 3 shows the RMS difference between retrieved 1 km layer mean temperatures and the collocated ECMWF forecast for all accepted cases as a function of retrieved effective cloud fraction. Results are shown for each of the lowest 8 km of the atmosphere. Agreement degrades with increasing cloud cover, but only very slowly except in the lowest 1 km of the atmosphere. RMS temperature differences from ECMWF at all levels are somewhat larger than the 1 K goal for retrieval accuracy. Part of this difference can be attributed to the fact that the ECMWF forecast is not perfect. It is also possible that the accuracy of the ECMWF forecast may be somewhat poorer with increasing cloud cover. The increase in RMS temperature differences at 0% cloudiness is somewhat misleading because a large percentage of clear cases occurred over Antarctica on this day.

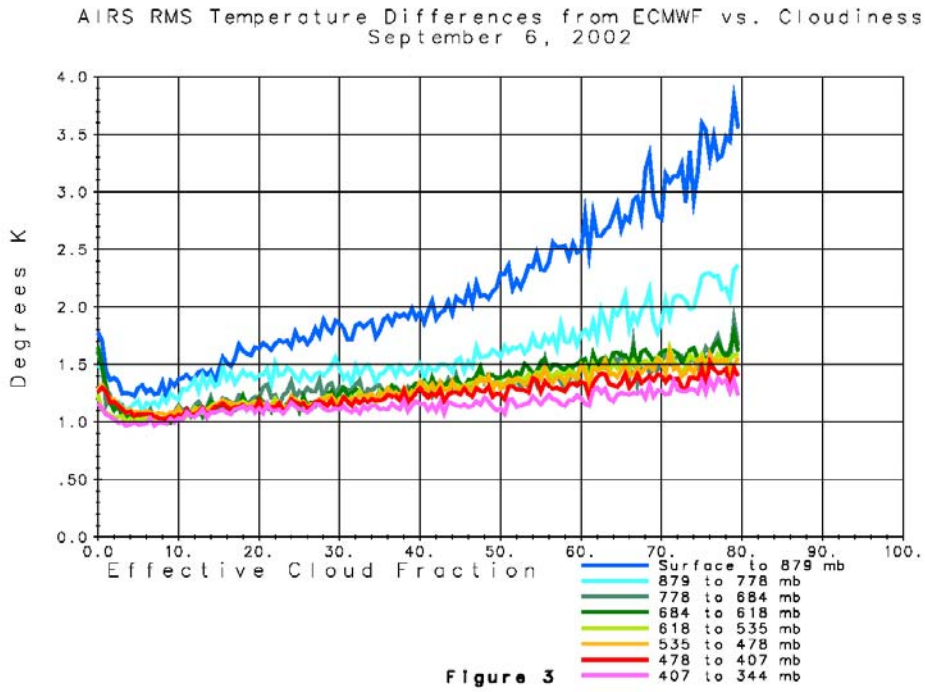

Figure 3

Figures 4a and 4b show RMS differences of temperature and moisture profiles from the “truth” with both simulated and real data. The gray and black curves reflect all accepted cases, and the pink and red curves are cases identified as clear, for simulated and observed radiances respectively. For temperature, 1 km layer mean differences from the truth are shown, and for water vapor, % differences in total integrated water vapor in 1 km layers are shown. In simulation, the truth is known perfectly, while with real data, the 3 hour ECMWF forecast is taken as a proxy for “truth”. For real data, as in simulation, temperature retrievals under cloudy conditions (roughly 66% of all cases are accepted) degrade by only a few tenths of a degree compared to cases identified as clear (roughly 8% of the cases are identified as clear), while water vapor retrievals do not degrade at all. Differences from “truth” are poorer with real data than in simulation. Two major causes of degradation are: 1) perfect physics was assumed in simulation; and 2) the “truth” has errors in real data. The degradation of soundings in the presence of “real clouds”, as compared to soundings in clear cases, appears to be similar to that implied by simulation.

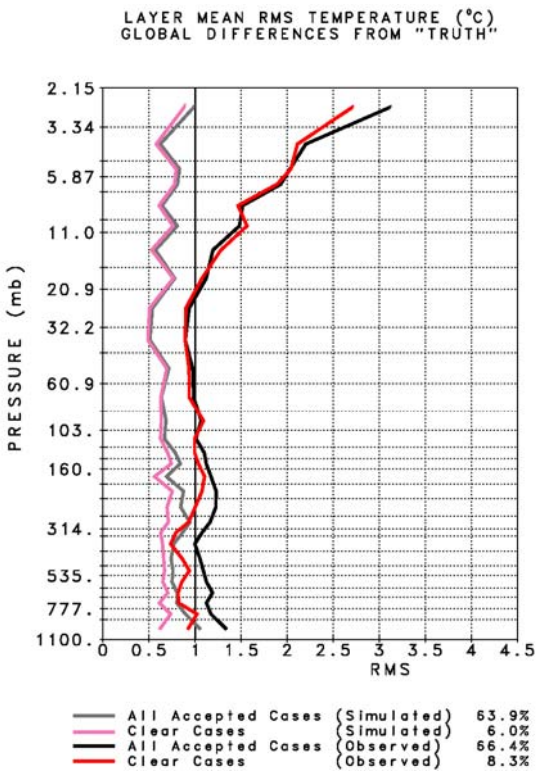

Figure 4a

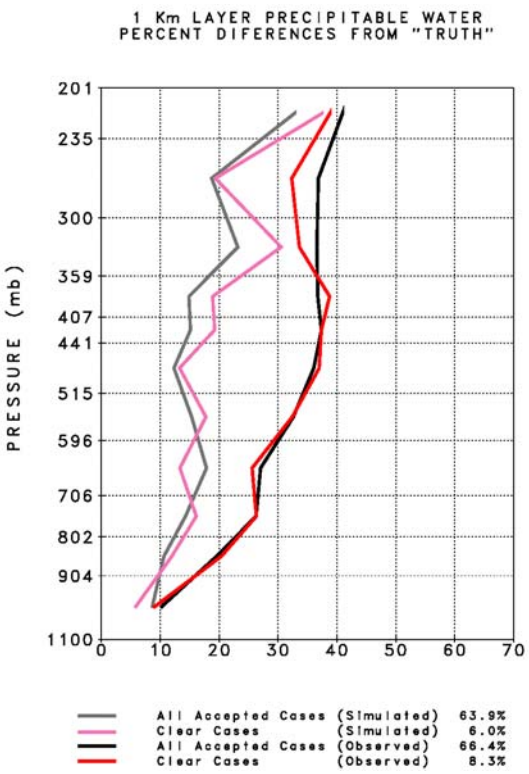

Figure 4b

Figure 5a shows RMS layer mean temperature differences between accepted retrievals, the ECMWF forecast, and collocated radiosonde reports (± 1 hour, ± 100 km) for September 6, 2002. The number of cases included in each of the layers is indicated at the right of the figure. It is interesting to note that the RMS temperature differences between the retrievals and ECMWF are generally smaller in the vicinity of radiosondes than they were globally (see Figure 4a). This is because the ECMWF forecast is more accurate in the vicinity of radiosondes than it is globally. The 3 hour ECMWF forecast agrees with radiosondes to 1 K between roughly 750 mb and 20 mb. Spatial and temporal sampling differences between ECMWF, retrievals, and radiosondes contribute to some extent to the increased differences between both ECMWF and retrievals as compared to radiosondes beneath 750 mb, as spatial and temporal variability of the atmosphere is greatest near the surface. Retrieval accuracy near radiosondes is somewhat poorer than that of the forecast at all levels, especially in the vicinity of 200 mb. This is most likely due to limitations in the current methodology used to account for systematic errors in the radiative transfer used in the calculations and accounting for residual physics errors in the channel noise covariance matrix. We expect further improvement in this area.

Figure 5b shows analogous results for percent differences in 1 km layer mean precipitable water, for which the sounding goal for AIRS is 20%. With regard to water vapor, it is clear that AIRS retrievals are significantly more accurate than the ECMWF forecast above 700 mb. AIRS differences from radiosondes are greater than the 20% goal. Spatial and temporal sampling differences between AIRS and radiosondes may contribute significantly to the apparent water vapor “errors” as water vapor changes rapidly in space and time.

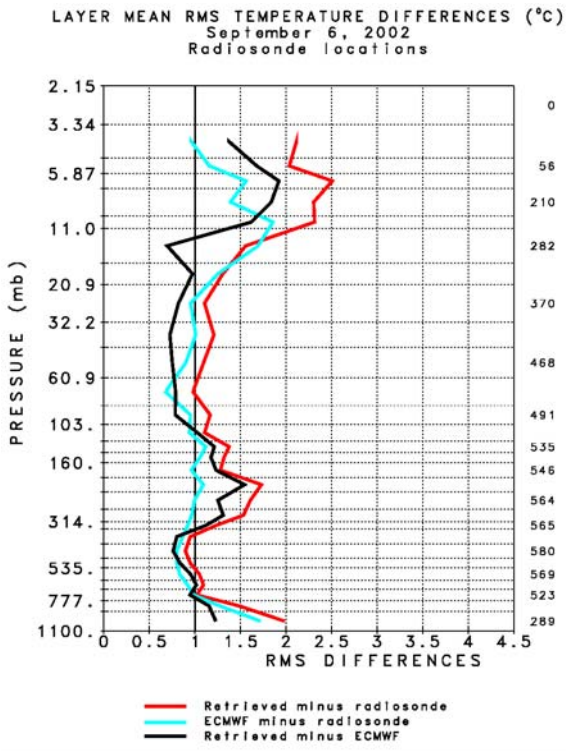

Figure 5a

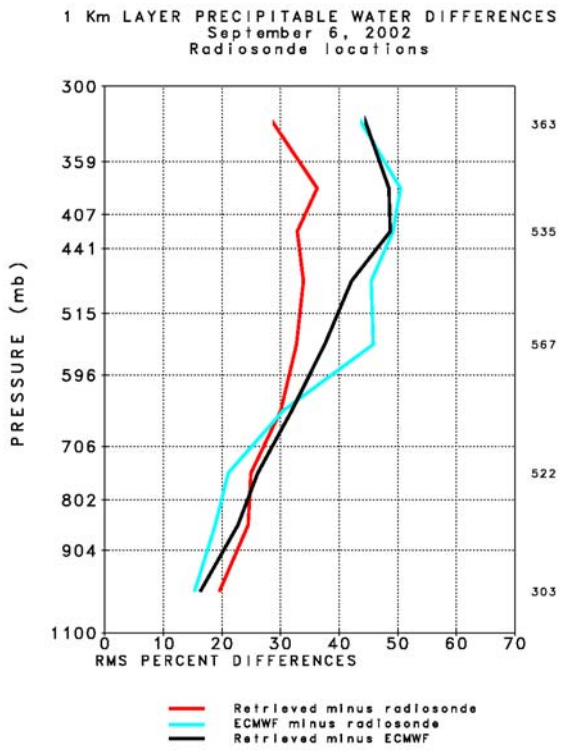

Figure 5b

Figure 6a shows the retrieved effective cloud top pressure and effective cloud fraction for ascending orbits on January 25, 2003. The results are presented in terms of cloud fraction in 5 groups, 0-20%, 20-40%, etc. with darker colors indicating greater cloud cover. These groups are shown in each of 7 colors, indicative of cloud top pressure. The reds and purples indicate the highest clouds, and the yellows and oranges the lowest clouds. Cloud fields are retrieved for all cases in which valid AIRS/AMSU observations exist. Gray means no data was observed. Figure 6b shows the retrieved 500 mb temperature field. Gray indicates regions where either no valid observations existed or the retrieval was rejected, generally in regions of cloud cover 80-100%. Retrieved temperature profile fields are quite coherent, and show no apparent artifacts due to clouds in the field of view. Figures 7c and 7d show retrieved values of total precipitable water vapor above the surface and above 300 mb. Note the high values of upper tropospheric water vapor to the east of extensive cloud bands attributed to cold fronts.

Figure 7a shows the retrieved 700 mb temperature field for ascending orbits on January 25, 2003. Figure 7b shows the collocated ECMWF 3 hour forecast 700 mb temperature field. These fields appear very similar to each other. Their difference is shown in Figure 7c, in which white shows agreement to ± 0.5K, each shade of red shows AIRS warmer than ECMWF in intervals of 1 K (0.5 – 1.5, 1.5 – 2.5, etc.), and each shade of blue shows AIRS colder then ECMWF in intervals of 1 K. The area weighted global mean difference of the two fields is 0.08 K, and the area weighted standard deviation is 1.13 K. Most areas are white or the first shade of red or blue. The largest differences between the two fields occur in the vicinity of 35°S – 55°S, 100°E – 140°E, and show up as a dipole,

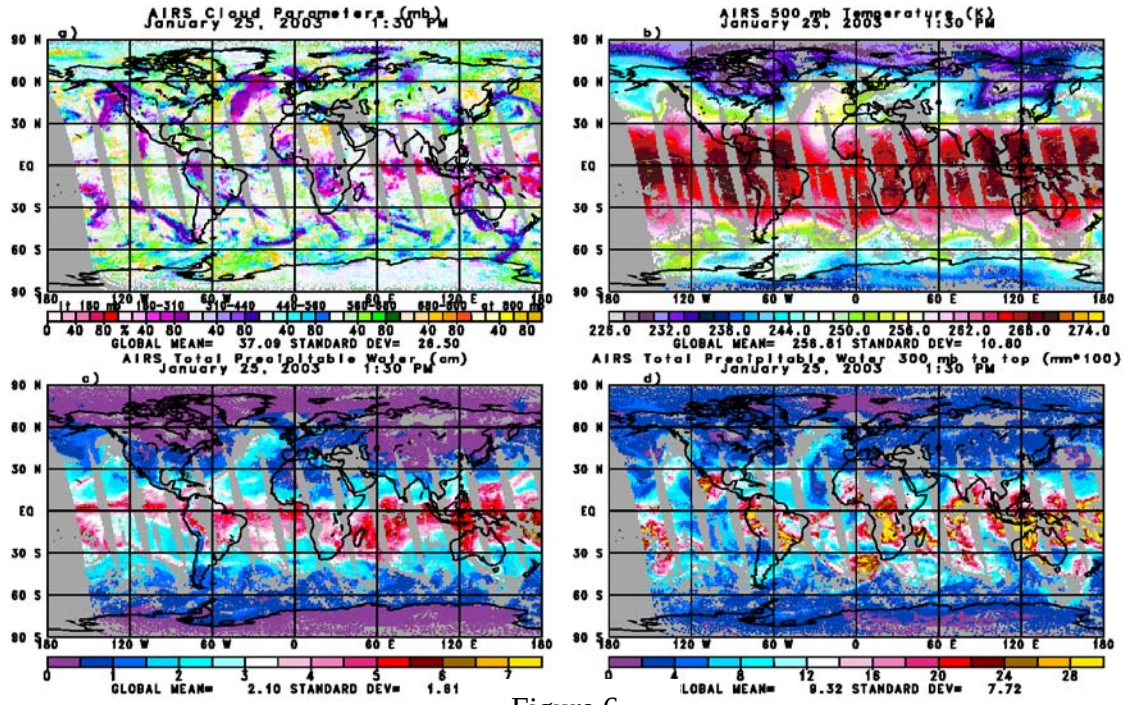

Figure 6

with AIRS warmer to the west of 120°E and colder to the east. Figures 7a and 7b show this to be an area of a cold air mass, extending from the polar region to the mid-latitudes. This cold air mass is coherent in both the retrieved and forecasted fields, but is centered further east in the retrieved field compared to the forecast field, corresponding to a phase error in the 3 hour ECMWF forecast. This is precisely the type of information that satellite data can provide (if accurate enough) to help improve forecast skill. Figure 7d shows the difference between the retrieved and forecast 100 mb temperature fields. At the 100 mb level, a corresponding warm front (not shown) exists in both the retrieved and forecast fields in the area discussed above, with an analogous phase error to that found at 700 mb. Consequently, the retrieved 100 mb field is cooler than ECMWF to the west and warmer to the east in the region discussed above. This out of phase relationship of patterns of differences from ECMWF at 700 mb and 100 mb is indicative of phase errors in the ECMWF forecast, as there is no reason for retrieval errors to be out of phase with each other at 700 mb and 100 mb. This out of phase relationship in spatial patterns of differences between retrieved and forecast temperatures at 700 mb and 100 mb is found in numerous places in Figures 7c and 7d and indicates many areas where the satellite data should improve the ECMWF forecast.

Forecast Impact Experiments

The data assimilation system used in the experiments is FVSSI which represents a combination of the NASA Finite Volume General Circulation Model (FVGCM) with the NCEP operational Spectral Statistical Interpolation (SSI) global analysis scheme implemented at lower than the operational horizontal resolution – T62. The basics of the finite-volume dynamical core formulation are given in DAO's Algorithm Theoretical Basis Document (see http://polar.gsfc.nasa.gov/sci_research/atbd.php), and the FVGCM has been shown to produce very accurate weather forecasts when run at high resolution.[5] The AIRS temperature profiles produced by SRT were presented to the SSI analysis as rawinsonde profiles with observational error specified at 1°K at all vertical levels.

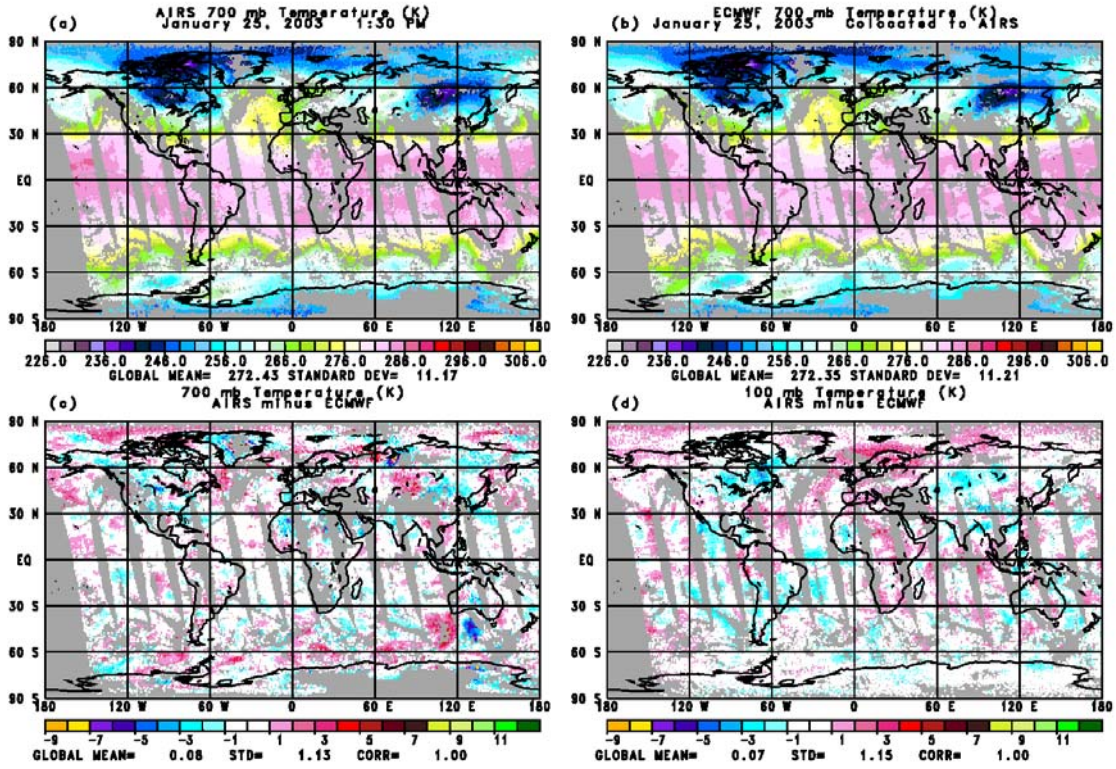

Figure 7

Results are presented for three sets of experiments in which data was assimilated for the period January 1 – January 31, 2003. Five day forecasts were run every two days beginning January 6, 2003 and forecasts every 12 hours were verified against the NCEP analysis, which was taken as "truth". In the first experiment, called "control", all the data used operationally by NCEP was assimilated, but no AIRS data was assimilated. The operational data included all conventional data, TOVS and ATOVS radiances for NOAA-14, 15, and 16, cloud tracked winds, SSM/I total precipitable water and surface wind speed over ocean, QuikScat surface wind speed and direction, and SBUV ozone profiles. In the second and third experiments, called "clear AIRS" and "all AIRS", temperature profiles retrieved from AIRS soundings were assimilated in addition to the data included in the "control" experiment. "Clear ocean" included all accepted temperature retrievals derived from AIRS over ocean and sea ice in cases where the retrieved cloud fraction derived from AIRS was less than or equal to 2%, while the "all ocean" experiment assimilated accepted AIRS temperature soundings over ocean and sea ice for all retrieved cloud fractions.

Figure 8 shows anomaly correction coefficients of forecast sea level pressure verified against the NCEP analysis for both Northern Hemisphere extra-tropics and Southern Hemisphere extra-tropics for both the "control" and "all AIRS" experiments. In the Northern Hemisphere, addition of all AIRS soundings resulted in an improvement in average forecast skill of the order of 1 hour or less, but an improvement in average forecast skill in the Southern Hemisphere on the order of 6 hours results from assimilation of AIRS soundings. Assimilation of AIRS soundings under essentially clear conditions (not shown), resulted in somewhat poorer forecasts than using all AIRS soundings. It should be noted that the

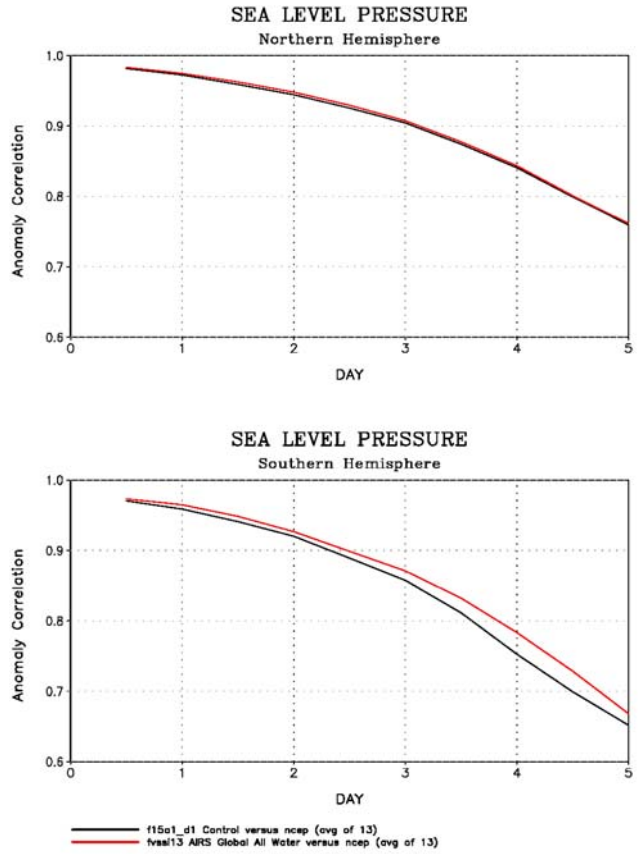

Figure 8

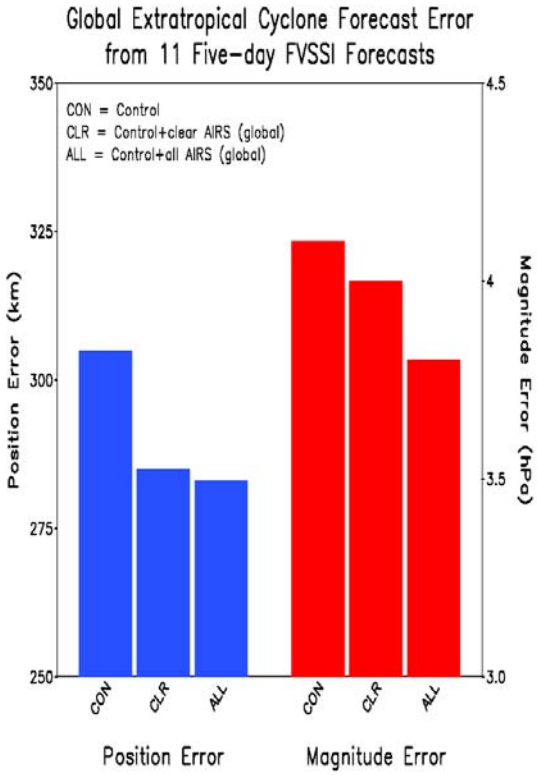

Figure 9

Aqua orbit (1:30 ascending) is almost identical to that of NOAA 16 carrying HIRS3, AMSU A and AMSU B, so AIRS/AMSU/HSB soundings are providing additional information to that contained in the AMSU A/AMSU B radiances on NOAA 16 in the same orbit.

Figure 9 shows the RMS position error (km) and magnitude error (hPa) for 5 day forecasts of extra tropical cyclones in the three experiments. It is apparent that addition of AIRS soundings improved RMS forecast skill for both the position and magnitude of extra-tropical cyclones globally, and addition of AIRS soundings in partially cloudy areas further improved forecast skill as compared to use of soundings only in essentially clear conditions.

Several thousand cyclones verifications are included in these statistics. Addition of AIRS data did not improve forecasted cyclone position and intensity for each cyclone. Some were improved substantially however. Figure 10 shows the impact of AIRS data on the 24 hour forecast of position and intensity of tropical storm Beni, which was centered roughly 4° east of New Caledonia on January 31, 2003 with a central pressure of 990 mb (see Figure 10d). The control forecast (Figure 10a) produced a relatively weak cyclone (1007 mb) displaced considerably to the northwest, while the 24 hour forecast using AIRS data (Figure 10b) was much more accurate in both position and intensity (995 mb). It is significant to note that our forecast using AIRS data was more accurate in both position and intensity than the NCEP operational forecast (Figure 10c) in this case, which, even though it used a higher resolution model and analysis system, did not have the benefit of AIRS data. The results shown indicate the potential of AIRS soundings to improve operational forecast skill. We are working with NCEP to arrange an experiment to add AIRS temperature soundings to an otherwise

equivalent run on the NCEP computing system to see the extent, if any, that operational forecast skill can be improved upon.

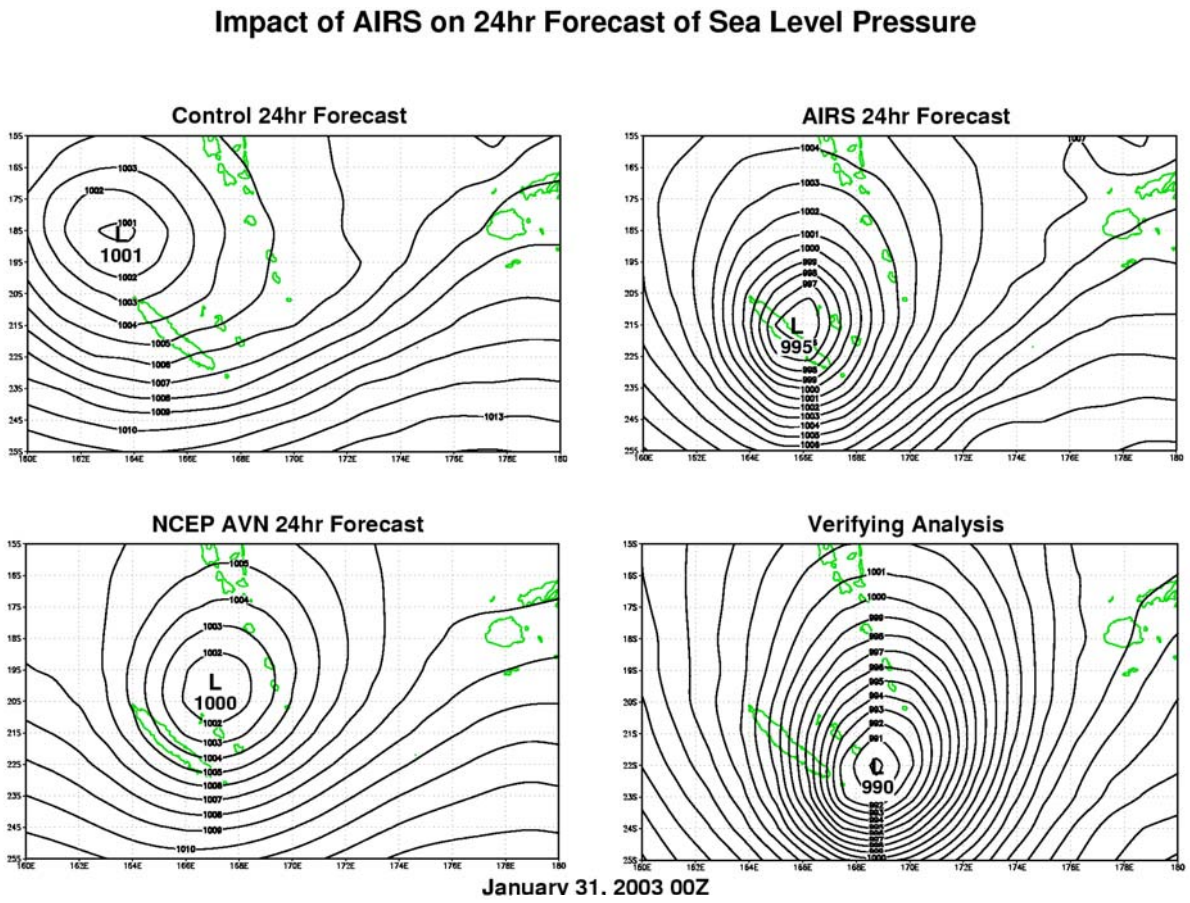

Figure 10

References

Pagano, T. S., H. H. Aumann, D. E. Hagan, and K. Overoye, February 2003. Prelaunch and in-flight radiometric calibration of the Atmospheric Infrared Sounder (AIRS). *IEEE Trans. Geosci. Remote Sensing*, **41**, 265-273.

Susskind, J., C. D. Barnet, and J. M. Blaisdell, February 2003. Retrieval of Atmospheric and Surface Parameters from AIRS/AMSU/HSB Data in the Presence of Clouds. *IEEE Trans. Geosci. Remote Sensing*, **41**, 390-409.

Rosenkranz, P. W., 2000. Retrieval of temperature and moisture profiles from AMSU-A and AMSU-B measurements. In *Proc. IGARSS*.

Goldberg, M. D., Y. Qu, L. M. McMillin, W. Wolff, L. Zhou, and M. Divakaria, February 2003. AIRS near-real-time products and algorithms in support of operational numerical weather prediction. *IEEE Trans. Geosci. Remote Sensing*, **41**, 379-389.

Lin, S.J., R. Atlas, and K. S. Yeh, January-February, 2004. Global weather prediction and high end computing at NASA. *Computing in Science and Engineering*, 29-35.